Switching Selectivity in Oxidation Reactions on Gold: The Mechanism of C–C vs C–H Bond Activation in the Acetate Intermediate on Au(111)

Cassandra G. F. Siler,[†] Till Cremer,[‡] Juan Carlos F. Rodriguez-Reyes,[‡,§] Cynthia M. Friend,[†,‡] and Robert J. Madix*[,†]

[†]School of Engineering and Applied Sciences and [‡]Department of Chemistry and Chemical Biology, Harvard University, 12 Oxford Street, Cambridge, Massachusetts 02138, United States

[§]Department of Industrial Chemical Engineering, Universidad de Ingeniería y Tecnología, Avenida Cascanueces 2221, Santa Anita, Lima 43, Peru

S *Supporting Information*

ABSTRACT: Carboxylates are important intermediates in oxidative reactions on gold, as they are precursors to carboxylic acids and CO_2; they may also act as site-blockers in oxidative coupling of alcohols, thereby decreasing both catalyst activity and selectivity. We demonstrate that the reaction selectivity and pathways for a prototype carboxylate, acetate, adsorbed on Au(111), are dramatically altered by the presence of coadsorbed atomic O. Finely tuning the initial oxygen coverage affords control of the product selectivity and the reaction pathway. Oxygen-assisted γ-C–H activation occurs with coadsorbed oxygen near 425 K, yielding mainly CO_2 and formaldehyde, and a kinetic isotope effect is observed for these products. In the absence of coadsorbed oxygen, acetate reacts at 530 K by C–C bond cleavage to form CO_2, methyl, and methyl acetate as well as minor products. These studies have led to the identification of a new synthetic pathway for ester formation, in which methyl (either produced in the reaction or introduced externally using methyl iodide) reacts with surface acetate to form methyl acetate. Detailed isotopic labeling studies using d_3-acetate, ^{13}C-acetate, and [18]O show that the methyl carbon forms mainly formaldehyde in the oxygen assisted reaction and methyl in the clean-surface reaction and that surface oxygen is incorporated into products in the low temperature, oxygen-assisted pathway. A complete mechanism is proposed and compared to the reaction of acetate on silver. These studies provide a detailed fundamental understanding of acetate chemistry on gold and demonstrate how the oxygen concentration can be used to tune selectivity.

KEYWORDS: *oxygen-assisted, C–H bond cleavage, acid–base, gold catalysis, methyl acetate*
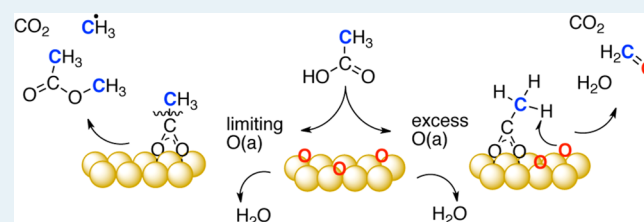
INTRODUCTION

Selective oxygen-assisted catalysis on gold has developed into a rich area of research, encompassing both reactor-based studies and model studies of reaction mechanisms and principles on single crystals. Oxygen-activated gold catalyzes selective oxidation of alkenes, alcohols, and amines,[1,2] forming epoxides,[3–6] aldehydes[7,8] or acids,[9–14] and imines,[15–18] respectively; oxidative coupling of alcohols yields esters,[16,19–25] and coupling of amines with aldehydes or methanol yields amides on gold.[17,26–31] Fundamental studies of these reactions have afforded insight into selectivity control as well as the prediction of new classes of reactions by gold cataly-sis.[21,25,30,32–34] In particular, mechanistic insight from ultra high vacuum (UHV) studies on Au(111) has been shown to directly correlate with activity seen on a nanoporous gold catalyst in a flow reactor.[21,25,33] Less well studied is the activation and oxidation of adsorbed carboxylates, which are often formed in oxidative processes along the pathway to combustion.

Carboxylates are important intermediates on gold because they (1) form as intermediates in oxidation reactions and (2) may lead to poisoning of a catalyst surface. Carboxylates are strongly bound to the surface and often form via secondary oxidation of hydrocarbons or alcohols. Acetate in particular has been implicated as the intermediate in nonselective oxidation of ethylene on silver[35,36] and of acetaldehyde and ethanol on gold.[22] Once formed, it has been proposed that carboxylates or similar intermediates may decrease catalyst selectivity by site-blocking,[37–39] thereby preventing desired reactions. In order to tailor reaction conditions to avoid these complications it is imperative to understand carboxylate stability and surface reactivity.

In general, oxidation reactions on gold are facilitated by adsorbed oxygen adatoms. Initially, oxygen atoms act as a

Brønsted base toward OH, NH, and even CH hydrogens to form the corresponding activated intermediate and adsorbed OH,[40,41] e.g., ethoxy forming from reaction with ethanol.[22] Further activation of *beta* C−H bonds leads to products, for example acetaldehyde and ethyl acetate from ethanol oxidation.[11,22,42] Density functional theory has predicted that the β-CH bond cleavage of methoxy via an oxygenate (an oxygen adatom, hydroxyl, or neighboring alkoxy) has a lower energy barrier than direct C−H activation by the metal.[43] In order to test this principle, we here address oxygen activation of *gamma* C−H bonds (Scheme 1), finding that C−H bond cleavage is facilitated via coadsorbed oxygen and that activation by the metal results in C−C bond cleavage at a much higher temperature.

**Scheme 1. Acetate and Ethoxy Adsorbed on a Surface**[a]
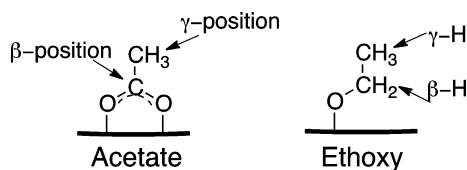
[a] γ and β positions are according to their position with reference to the surface.

Herein, we demonstrate that coadsorbed oxygen opens new reaction pathways for acetate on Au(111), leading to a selectivity switch. In conjunction, the stability of acetate on Au(111) is decreased by coadsorbed oxygen due to the opening of pathways involving O attack.[44] A detailed mechanism for reaction of acetate both in the presence and absence of adsorbed atomic oxygen is established using temperature-programmed reaction spectroscopy and isotopic labeling experiments. In addition, a new synthetic route for esters via carboxylates was discovered in which methyl introduced externally or produced during the reaction is added to acetate on the surface, forming methyl acetate. These studies demonstrate the key roles of adsorbed O in determining reactivity on gold and suggest a means of controlling selectivity in catalytic systems that produce carboxylates.

■ RESULTS

The effect of coadsorbed atomic oxygen on acetate reactivity was first investigated by varying the amount of acetic acid exposed to a surface with a fixed concentration of atomic oxygen of 0.2 monolayers (ML). Acetate is formed from reaction with O adsorbed on Au(111) through the well-established acid−base chemistry on oxygen-covered gold:[41]

$$O_{(a)} + 2CH_3COOH_{(g)} \rightarrow H_2O_{(a/g)} + 2CH_3COO_{(a)} \quad (1)$$
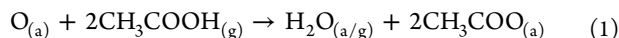
Excess acetic acid was dosed onto a Au(111) surface with an initial oxygen coverage of 0.2 ML at 200 K − the conditions being chosen to prevent the buildup of either water or acid multilayers. With this procedure, the reaction goes to completion, and acetate was formed free of coadsorbed oxygen atoms. In contrast, with a small initial dose of acid at the same initial oxygen coverage, excess adsorbed oxygen remained (Figure 1).

Coadsorbed oxygen initiates a reaction inaccessible in its absence, facilitating C−H bond cleavage and reaction at a much lower temperature with a decidedly different distribution of products compared to the oxygen-free surface. Reaction of
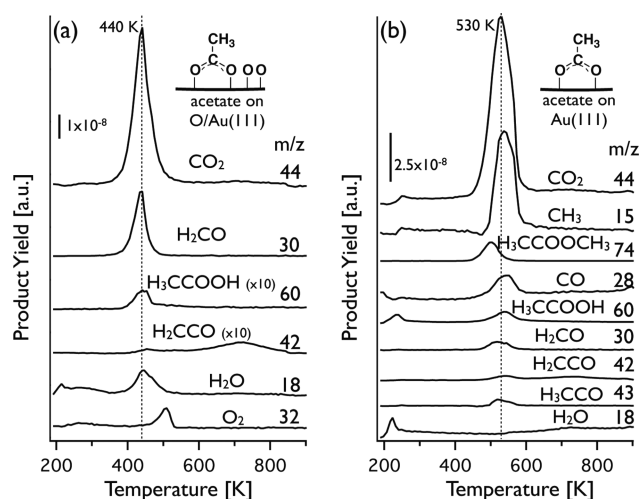

Figure 1. Temperature-programmed reaction spectra of acetate in the presence and absence of coadsorbed oxygen. Initial oxygen coverage in both cases was 0.2 ML O. Acetic acid was dosed at 200 K (a) with the acid dose controlled to retain excess oxygen and (b) in excess acid to consume all oxygen. Unless otherwise noted, products are scaled to reflect their relative yields, calculated using quantitative mass spectrometry methods described in the Experimental Methods and the Supporting Information.

acetate under the two conditions, as measured by a temperature-programmed reaction, occurred at 440 and 530 K, respectively, corresponding to activation energies of 29 and 35 kcal/mol (the analysis was simplified by assuming first order reaction and a pre-exponential factor of 10^{14}). The pre-exponential factor of 10^{14} was chosen because it is typical of experimentally determined pre-exponential factors of similar intermediates,[45,46] lying in the middle of the range for similar H-elimination reactions, which range from 10^{12}–10^{16}.[47−49] Previously, we used the value of 10^{16} in calculations for acetate on gold, which results in an upward shift of ~3−5 kcal/mol.[44] The reaction temperature drops even further, to 400 K ($E_a = 26$ kcal/mol), with initial oxygen coverages ≥0.3 ML (see below). CO_2 is the main product for both reaction pathways; however, there are significant differences in the other products.

The product distributions are strongly dependent on whether there is excess oxygen on the surface (Figure 2, Table S1). With excess oxygen the major products are carbon dioxide and formaldehyde, with minor amounts of acetic acid, ketene (H_2CCO), water, and a small amount of carbon monoxide. Products are evolved concomitantly with the CO_2 (Figure 1) with the exception of a broad ketene peak around 700 K. In the absence of excess oxygen several new products form: methyl, methyl acetate, and carbon monoxide along with minor amounts of formaldehyde, H_3CCO radical, acetic acid, ethane, and ketene. Yields for minor products and selectivities for all products are included in Table S1. The production of methyl acetate indicates a new synthetic route for esters using acetate as a synthetic reactive intermediate (see below). Quantitative analysis of the data was used to identify products and determine the relative amounts formed for both reaction conditions.

The changes in selectivity and kinetics can also be monitored by varying the initial oxygen coverage while consistently dosing an excess of acetic acid. This way, the capacity of the surface dictates when coadsorbed oxygen remains on the surface, which in turn controls the reaction pathway. The preferred reaction pathway transitions in a narrow window of initial oxygen, 0.24−
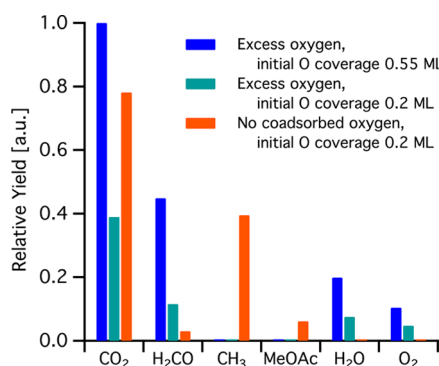
Figure 2. Relative yields for major products of acetate reaction (CO_2, H_2CO, CH_3, methyl acetate, H_2O, and excess oxygen) under varying reaction conditions, calculated using quantitative mass spectroscopy, with an enhancement factor of 3.2 included for CH_3. Yields are normalized to the amount of CO_2 produced for an initial oxygen coverage of 0.55 ML. Calculation details in the Experimental Methods and the Supporting Information.

0.3 ML. (Figure 3). Starting at the lowest oxygen coverage, the high temperature CO_2 peak (530 K) grows in; at 0.24 ML O
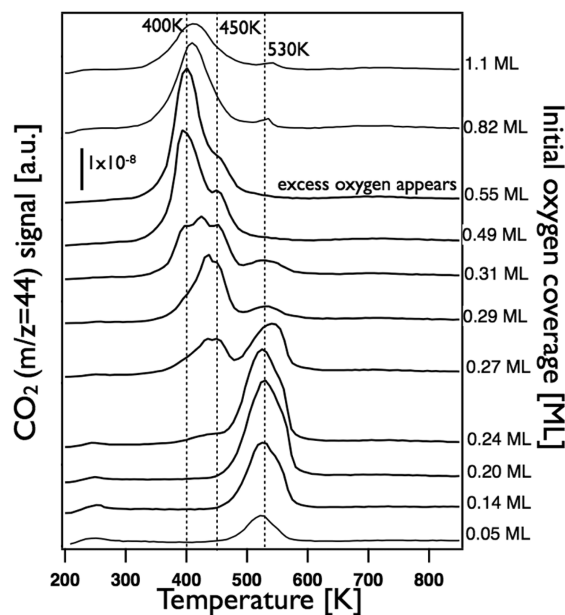

Figure 3. Multiple low temperature reaction pathways for acetate activation evolve with increasing amounts of coadsorbed oxygen on the surface, as marked by CO_2 traces for acetate reaction for excess acetic acid dosed at 200 K on varying O-precoverages on Au(111). CO_2 is the main product in all cases. Excess oxygen recombines at ~540 K and is present at initial oxygen coverages of 0.55 ML and higher.

the low temperature peak (~450 K) starts to form; at 0.3 ML O the lowest temperature peak (400 K) builds in and becomes dominant at 0.5 ML O, although the 450 K peak is still present as a shoulder. Although excess oxygen after the reaction is not seen, water forms with CO_2 during the reaction, which is evidence of coadsorbed oxygen reacting with hydrogen from the acetate. Above 0.5 ML O, unreacted oxygen recombines to form O_2, and the amount of CO_2 formed decreases; the latter effect is attributed to reduction in the binding capacity for the acetate.

The kinetics for CO_2 production is also strongly dependent on the initial O coverage and whether there is excess O adsorbed on the surface (Figure 3). Specifically, the peak temperature for CO_2 is much higher when there is not excess adsorbed oxygen. Based on the decrease in peak temperature for CO_2, the 6 kcal/mol activation energy difference seen at 0.2 ML O with excess oxygen (see Figure 1a) increases to 9 kcal/mol at initial oxygen coverages ≥0.3 ML.

The mechanisms for CO_2 formation are changed by the presence of adsorbed excess O, accounting for the different peaks in the temperature-programmed reaction data (Figure 3). The rate-limiting step for *oxygen-assisted* formation of CO_2 formation at low temperature involves C−H bond cleavage based on the kinetic isotope effect observed for reaction of d_3-acetate (Figure 4). In contrast, the peak temperature of the
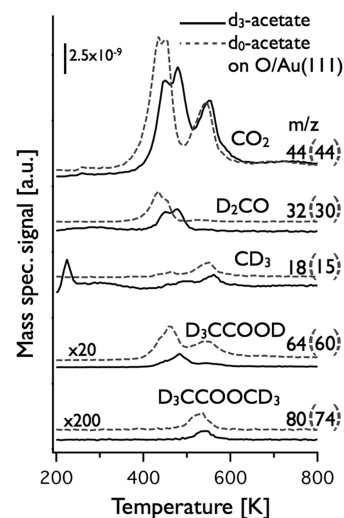

Figure 4. Deuterium isotopic labeling experiments for selected products on a 0.2 ML O/Au(111) surface using an acetic acid dose that allows both the low temperature and high temperature pathways to be observed. d_4-Acetic acid was dosed at 200 K to form the d_3-acetate. d_3-Acetate data is shown in black; gray dashed lines are data obtained separately for d_0-acetate.

higher temperature route that occurs in the absence of excess O is the same for d_0- and d_3-acetate. At an initial oxygen coverage of 0.2 ML O and an acid dose for which both the low temperature and high temperature peaks are observed, the effect of isotopic substitution for both reaction channels can be observed (Figure 4). For the oxygen-assisted reaction channel, a temperature shift of 15 K to higher temperature is observed for CO_2 and formaldehyde production from d_3-acetate relative to the perhydrido acetate, indicating that C−H bond activation is involved in the rate-limiting step. In the high temperature route there is no measurable temperature shift for CO_2 production, and both methyl and methyl acetate are completely deuterated. These data are unequivocal evidence that the high temperature reaction pathway involves C−C bond cleavage and that the methyl group (resulting from the C−C bond cleavage) can either react with another acetate to form methyl acetate or desorb intact from the surface.

Surface oxygen is incorporated into the products in the oxygen-assisted, low temperature route, as shown by ^{18}O-labeling of the surface oxygen (~35% [18]O, Figure 5). The most significant amount of [18]O incorporation is into formaldehyde evolved at 400 K. The higher temperature formaldehyde peak
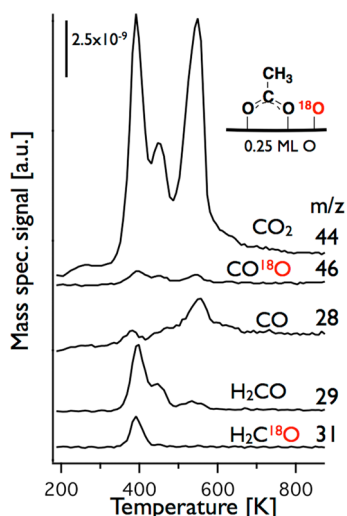
Figure 5. Surface oxygen incorporation into products is shown by reaction with $^{18}O/Au(111)$ (35%). ^{16}O is replaced by ^{18}O by dosing $H_2{}^{18}O$ for 30 s at 180 K on 0.3 ML $^{16}O/Au$ and then flashing to 350 K to desorb the water. The final oxygen coverage is about 0.25 ML (35% ^{18}O). The acetic acid dose was controlled in order to observe both reaction channels.

(530 K), however, does not contain ^{18}O, indicating that it is formed via a different route. A small amount of ^{18}O appears in the higher temperature channel, incorporated into CO_2. A small amount of ^{18}O (~7% of products contain one ^{18}O) is incorporated into the acetic acid and methyl acetate (not shown), indicating that the adsorbed acetate undergoes a limited amount of exchange with oxygen on the surface, consistent with previous studies.[50] In neither the low or high temperature pathways is ^{18}O incorporated into the CO.

The differences in reaction pathways as a function of oxygen coverage are also demonstrated using ^{13}C-labeling of the methyl group to delineate which products originate from the methyl carbon (Figure 6). In the O-assisted pathway ($\theta_{initial}$ = 0.5 ML), formaldehyde is 100% ^{13}C-labeled. This result in combination with the incorporation of ^{18}O from the surface (Figure 5) shows that formaldehyde is produced from attack of
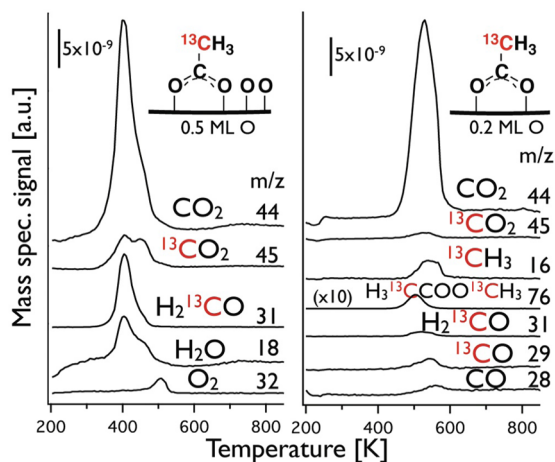

Figure 6. Reaction of ^{13}C-acetic acid ($^{13}CH_3COOH$) on Au(111) with initial oxygen coverages of 0.5 ML O (left) and 0.2 ML O (right). Multilayers of acetic acid were dosed at 200 K on both oxygen coverages.

the methyl carbon by adsorbed oxygen. Some total oxidation of the methyl group also occurs, based on the fact that ~18% of the CO_2 is also ^{13}C labeled. In the absence of excess O, $^{13}CH_3$ and $^{13}CH_3-C(=O)^{13}CH_3$ (methyl acetate) are formed. The methyl acetate is 100% doubly labeled, which supports the conclusion that the methyl is also 100% labeled, although an exact number for the methyl is difficult to assess because of overlapping fragments with other products. Only ~3% of the CO_2 is ^{13}C-labeled. This experiment was also used to confirm that neither ethane nor ethylene was formed as a major product in the high temperature route (Figure S1).

We further probed the reaction to form methyl acetate by using an external source of methyl (CH_3I) to demonstrate that the methyl acetate is produced by addition of methyl to an intact acetate species. Acetate was first isolated on the gold surface by dosing acetic acid on 0.1 ML O at 200 K, followed by exposure to methyl iodide at 140 K. Methyl iodide is known to dissociate on Au(111) starting at 150 K, reacting a coverage of 0.054 ML upon heating to 300 K.[51] In these experiments, methyl acetate (monitored using the major fragment, $m/z = 43$, as well as the parent ion, $m/z = 74$) forms via reaction of acetate with adsorbed methyl from 200 to 300 K (Figure 7). At
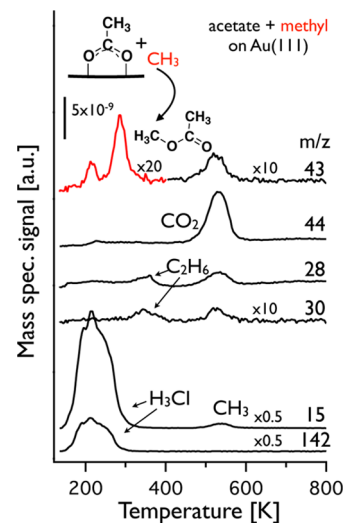

Figure 7. Acetate reacts with an external methyl from methyl iodide to form methyl acetate below room temperature. Acetic acid was dosed at 200 K on 0.1 ML O/Au(111), then annealed to 265 K, and cooled back down to 140 K. Methyl iodide was introduced in excess at 140 K. The low temperature m/z 15 and 142 are molecular methyl iodide.

higher temperature, methyl acetate is formed via acetate decomposition at 530 K. The m/z 28 and 30 peaks at 350 K are due to ethane formation from methyl recombination.[52] This experiment clearly demonstrates the principle for facile ester formation using an alkyl source for addition to the adsorbed carboxylate.

■ DISCUSSION

Four fundamental principles important in heterogeneous oxidation catalysis emerge from this study: (1) The selectivity for acetate reaction is determined and tuned by the presence or absence of coadsorbed oxygen; (2) adsorbed oxygen atoms activate the gamma-CH bond (Scheme 1) destabilizing the acetate intermediate; (3) in the absence of adsorbed oxygen, acetate decomposition is rate-limited by the C−C bond rupture at higher temperature; (4) methyl addition to the acetate

provides a direct route to formation of the corresponding ester. The reaction mechanisms for each pathway and effects of oxygen coverage are discussed below and compared to the carboxylate chemistry on silver and copper. These principles serve as a guide for selecting conditions for catalytic reactions that involve acetate as an intermediate. The correspondence between fundamental studies on O/Au(111) and reactions under flow conditions at atmospheric pressure using nano-porous gold catalysts has already been demonstrated in our lab.[21,25,33]

Coadsorbed Oxygen and C−H Bond Cleavage. The activation energies of the oxygen-assisted and gold surface mediated reaction differ by 6−9 kcal/mol, as the coadsorbed oxygen opens a new, lower-energy reaction pathway. This suggests possible strategies for operating or purging catalysts that may be poisoned by the buildup of adsorbed carboxylates, that is, maintaining a slight excess of oxygen in the feed stream in order to enable lower-temperature reaction of the carboxylate molecule.

The facile activation of the gamma C−H (γ-CH) bond in adsorbed acetate by coadsorbed oxygen suggests that a similar process may occur for the beta C−H bond (β-CH) in oxygen-assisted coupling reactions. β-H elimination takes place in most oxidative processes on gold, forming aldehydes and esters, among other products, and has been predicted by theory to be facilitated by adsorbed oxygen, hydroxyl, or alkoxies.[43] However, because β-CH cleavage is so facile, it is difficult to prove experimentally whether this is the case. Gamma C−H bonds are more stable than those located beta to the surface, because they lack proximity to an electron-withdrawing atom (Scheme 1). Indeed, we have shown that coadsorbed oxygen is necessary for low temperature γ-CH cleavage, and as shown by the observed kinetic isotope effect of 6.9,[44] the oxygen-assisted route was indeed limited by γ-CH bond breaking. While it is theoretically possible that an even higher temperature may allow for direct γ-CH activation by the surface, it was not accessible in our experiments, as C−C bond cleavage and complete removal of acetate took place before any direct γ-CH activation by the metal.

On coinage metals, adsorbed oxygen exhibits a pattern of facilitating γ-CH bond breaking. The most direct comparison to acetate on gold is acetate on silver. On Ag(110), acetate reacts with coadsorbed oxygen as low as 340 K to form formate, which decomposes to CO_2 and H_2 at 400 K.[53] Sault et al. invoke a mechanism that involves direct γ-H activation of the methyl carbon and subsequent reaction of the activated CH_2 group to form formate. Interestingly, formaldehyde is not observed, whereas it is on O-covered Au(111). On clean Ag(110), acetate decomposition does not occur until 580 K, where CO_2, CH_4, acetic acid, and ketene form, similar to reaction on clean Au(111).[36] *tert*-Butoxy, which also possesses only γ-C−H bonds, exhibits a similar pattern of oxygen-assisted reactivity on Ag(110); the oxygen-assisted reaction takes place at 440 K, while reaction on the clean surface occurs at 510 K.[54] On copper, however, reactions of *tert*-butoxy occur around 600 K, with only a slight shift to lower temperature when oxygen is present.[55] In all cases the oxygen-assisted reaction has a significant kinetic isotope effect, indicating that C−H bond breaking is the rate-limiting step. While copper, silver, and gold all have the mechanism of γ-C−H bond breaking by coadsorbed oxygen, only silver and gold exhibit this pronounced change in stability, manifested by the reaction

temperature shift of over 100 K, between the clean and oxygen-covered surfaces.

Coverage Effects. The product distributions depend strongly on the oxygen coverage, and a sudden switch in selectivity takes place due to a very slight change in initial oxygen coverage, just below 0.3 ML O (Figure 8). CO_2 is the
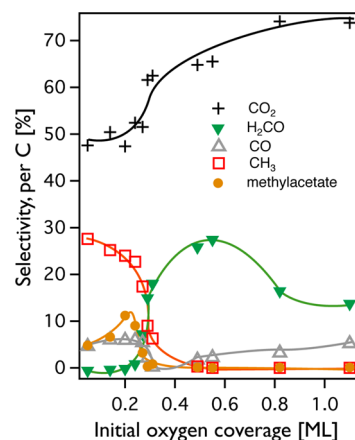

Figure 8. Selectivity (on a per carbon basis) for acetate reaction as a function of initial surface oxygen coverage shows a sharp change in product distribution at ∼0.3 ML initial O coverage. Corresponding yield is shown in Figure S3. For details on the calculations on the yield and selectivity, see the Supporting Information. The curves serve as a guide and do not correspond to a fit of the data.

dominant product at all initial oxygen coverages, but the other products differ significantly. The products occurring exclusively in the high temperature channel, methyl and methyl acetate, reach their peak yield at 0.2 ML O (corresponding to 0.4 ML of acetate), indicating that, above this coverage, coadsorbed oxygen begins to be present, in agreement with the CO_2 peak shift in Figure 3. Formaldehyde yield, which is most uniquely characteristic of the oxygen-assisted reaction pathway, peaks at 0.55 ML O. Total conversion of acetic acid also depends on oxygen coverage and peaks when the maximum amount of acetate is formed on the surface, at both ∼0.2 and 0.55 ML initial oxygen coverages. At higher oxygen coverages the total product yield decreases, apparently due to site limitations for acetate formation, as reflected by the increase in oxygen recombination above this coverage.

The amount of oxygen coadsorbed with the acetate dictates the products formed at 530, 450, and 400 K, respectively, with a pronounced further lowering of the peak temperature of the oxygen-assisted reaction at an initial coverage of ≥0.3 ML O (Table 1). Possible factors that could contribute to this phenomenon include the following: (1) a change in the dominant type of oxygen on the surface as the coverage increases, (2) repulsive lateral interactions among adsorbed acetate due to closer packing, and (3) a change in the binding of the acetate, perhaps to monodentate, causing it to react with oxygen at lower temperature. Because of the fact that both the

**Table 1. Comparing Surface Coverage to Reaction Pathway**

initial oxygen coverage (ML)	dominant reaction temp	coadsorbed O (ML)
0.05−0.24	530 K	none
0.27−0.31	440 K, 530 K	0.12−0.16
0.49−1.1	400 K	0.28−0.69

Scheme 2. Reaction Mechanisms for Both the Clean-Surface and Oxygen-Assisted Reaction Pathways for Acetate on Au(111)

(a) Clean-surface reaction mechanism
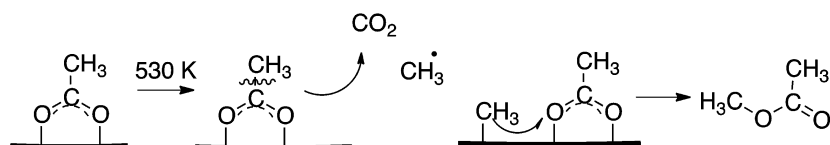
(b) Oxygen-assisted reaction mechanism
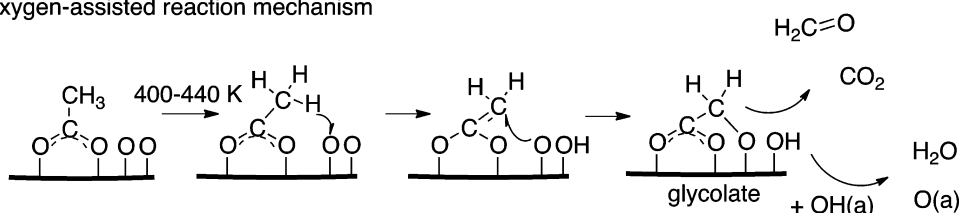
oxygen structure and the coverage change as the surface is heated during the reaction, these effects are very difficult to separate. Notably, the shift of the lower temperature peak to 400 K only occurs when the combined coverage of acetate and coadsorbed oxygen is high (above 0.8 ML, see Table S2). This suggests that the shift arises from either a structural change or strong intermolecular interactions for a densely packed layer.

Reaction Mechanisms. The switch in selectivity for acetate reaction on Au not only demonstrates how the product distributions can be tuned by adjusting the steady-state oxygen coverage in a catalytic process (for example by changing the oxygen partial pressure) but also suggests a new route for production of esters (Scheme 2).

Clean-Surface Pathway (530 K), Scheme 2a. In the absence of coadsorbed oxygen the decomposition of the acetate occurs through C−C bond activation by gold, yielding CO_2, methyl, methyl acetate, and CO as the main products (Figure 2). Because gold does not activate C−H bonds, the C−C scission occurs selectively at elevated temperatures. This led to the discovery of a different pathway for methyl ester formation— addition of methyl to one of the acetate oxygens. In the initial stages of reaction, there is intact acetate that reacts efficiently with the methyl to form methyl acetate. In a catalytic process, the conditions for selective C−C dissociation could be achieved by maintaining a low steady-state rate of O_2 dissociation relative to the rate of acetate formation by adjusting the partial pressures of reactants.

The order of appearance of the products demonstrates clearly that C−C dissociation is the first step in the reaction of acetate on the clean gold surface (Figure S3). Specifically, CO_2 and methyl acetate peak onset begins at 460 K indicating that C−C bond rupture is the first step, yielding CO_2 and CH_3 (Scheme 2a). Once the surface is depleted of acetate, gas phase methyl is evolved. Surface lifetimes of radical species have been measured to be on the order of 10^{-8} s on Mo(110), giving sufficient time for reaction with nearby acetates initially.[56] The observation of a minor amount of ethane is also evidence for the finite lifetime of adsorbed methyl groups. The other products begin desorbing at 490 K, indicating the onset of C− O bond cleavage. Formation of H_3CCO is direct evidence for C−O bond dissociation as well as minor products requiring $O_{(a)}$. Formed through the C−O bond cleavage, $O_{(a)}$ can attack a methyl group, resulting in γ-C−H bond activation to form small amounts of formaldehyde or even CO_2 in much the same

way as the low temperature oxygen-assisted reaction. The minor products mechanisms are shown in Scheme S1.

Oxygen-Assisted Pathway (400−440 K), Scheme 2b. Under O-rich conditions, adsorbed oxygen attacks the methyl group of the acetate leading to γ-CH activation and OH formation. This is demonstrated by the kinetic isotope effect observed for deuteration of the methyl group (Figure 4). After γ-hydrogen activation another oxygen can react with the activated CH_2−moiety, ultimately forming formaldehyde and CO_2. An alternative mechanism would be for adsorbed oxygen to attack the methyl carbon, causing C−C bond cleavage to form adsorbed methoxy. However, methyl formate, which is the characteristic product of methoxy on gold,[20] is not observed. Therefore, γ-CH activation and attack at the carbon center must lead directly to formaldehyde. We propose the formation of the glycolate intermediate, which is the same intermediate proposed for acetate reaction with oxygen on silver.[53] Cleavage of the glycolate C−C bond then leads to formaldehyde and CO_2. However, the stoichiometry requires another channel for CO_2 formation (Table S1, Figure 8). As reflected in the ^{13}C data, some of the acetate methyl undergoes further H-activation to form CO_2 (Figure 6). This could occur either by C−H activation of the glycolate intermediate or by secondary oxidation of the formaldehyde.

Comparison with Reactivity of Silver. The reactions of acetate on metallic gold and silver show interesting similarities and important differences. Most significantly, coadsorbed oxygen lowers the activation energy for acetate reaction on both metallic silver and gold, as manifested by the reaction temperature decreasing by well over 100 K as compared to reaction on the clean surfaces. In both cases, direct oxygen attack by adsorbed oxygen on the γ-H accounts well for the reactions observed. The main carbon-containing product of the oxygen-assisted reaction on both surfaces is CO_2. On silver the CO_2 originates from both the methyl and carboxyl carbons in separate, successive steps via conversion of the methyl to adsorbed formate,[53] whereas on gold, CO_2 is formed primarily from the carboxyl carbon, with the methyl carbon forming primarily formaldehyde, even in the presence of excess oxygen. A glycolate intermediate is proposed on both surfaces, yielding formate and CO_2 on Ag and formaldehyde and CO_2 on Au. The explanation of this difference lies in the details of the activation energies and transition states during the attack of adsorbed oxygen on the methylenic carbon in the glycolate. If

the interaction between adsorbed oxygen with this carbon is weaker on the gold surface it could be viewed as perturbative, leading to C—C bond rupture and formaldehyde release, whereas a stronger interaction would lead to C—O bond formation resulting in adsorbed H_2CO_2, which is known to convert to formate. Further exploration of the energetics of these reaction pathways may be possible using density functional theory but is beyond the scope of the present study.

On the clean surface, it is clear that on both silver and gold, the C—C bond breaks, forming either methyl (gold) or methane (silver). This difference could be due to the inherent ability of silver (and inability of gold) to break C—H bonds and provide adsorbed hydrogen atoms, as the observed carbon deposition on silver is evidence for the liberation of hydrogen, which combines with methyl to form methane.[36] On gold, however, neither carbon deposition nor hydrogen evolution was detected; hence, there is no adsorbed atomic hydrogen with which to react to form methane. Further, no methyl acetate was observed on silver; however, it is not known if this product was examined in the earlier work.

Patterns of reactivity have powerful abilities of prediction for catalytic activity. This study further develops the paradigm for oxygen-assisted reactions, establishing reaction principles for carboxylates on gold. Subtle differences in binding energy for the intermediates on gold and silver involved in these reactions lead to differences in reaction products, underscoring the necessity of accurate calculations for predicting relative rates of branching processes in catalytic reactions.

CONCLUSIONS

We have clearly established a pattern of low-temperature oxygen-assisted γ-C—H activation for carboxylates on gold and silver. The implications of this are two-fold. First, coadsorbed oxygen significantly destabilizes adsorbed carboxylates on these metals by introducing a new, lower energy reaction pathway. On both silver and gold carboxylates have been implicated in surface site-blocking, thereby decreasing catalyst selectivity. By using these principles of oxygen-assisted reaction, it may be possible to decompose the unwanted carboxylates at lower temperature. Second, γ-CH activation is facile and selective when done directly by coadsorbed oxygen. This suggests, along with theory, that the same mechanism may be operative in selective, low-temperature β-CH activation on gold.

In the absence of oxygen, however, acetate undergoes C—C bond cleavage by the gold surface at higher temperature. An exciting outcome of this work is the discovery of a new route for methyl acetate synthesis. New, more complex ester formation via carboxylates may be possible with knowledge of this new reaction pathway involving direct addition of alkyls to adsorbed carboxylates on gold.

EXPERIMENTAL METHODS

Temperature-programmed reaction spectroscopy (TPRS), which has been described in detail elsewhere,[57] was done in an ultra high vacuum chamber with a base pressure of ~2 × 10^{-10} Torr using a triple filter Hiden quadrupole mass spectrometer (HAL-Hiden/3F). The heating rate in all experiments was 5 K/s. To prevent electron-stimulated reactions from taking place due to the mass spectrometer filament, a bias of −100 V was applied to the sample during TPRS experiments. The gold (111) single crystal was cleaned by argon ion sputtering and annealing to 900 K, followed by

multiple oxidation cycles using ozone until no CO_2 desorbed from the surface. Ozone was generated using a commercial ozone source (LG-7 CD Laboratory Ozone Generator). Approximately 15 g/Nm^3 ozone in oxygen was constantly flowed through a gas line from which the ozone was dosed, creating adsorbed atomic oxygen on the surface. Each day, the ozone dose was calibrated using a reference saturation coverage of 1.1 ML. Acetic acid was dosed using a direct doser, and doses were controlled by number of turns of the dosing valve; a background pressure rise was not observed during the acid doses.

To identify the products in each case, a rigorous method of quantitative TPRS was applied, which accounts for the mass fragments of all the species.[24] The product identities were deciphered using fragmentation patterns from neat samples or the NIST database when neat samples were unavailable and confirmed by isotopic labeling. To calculate the yield for each product, the ionization cross section, quadrupole transmission and detection coefficients, and fragmentation patterns were taken into account. The correction factors applied are included in the Supporting Information, Tables S2, S3, and S5. A MATLAB code was developed for the quantitative TPRS analysis. It is available on the Friend group Web site under "Resources" (http://faculty.chemistry.harvard.edu/friend-lab).

ASSOCIATED CONTENT

Ⓢ Supporting Information

Table of relative and percent yields for acetate reaction on 0.55 ML O and 0.2 ML O with and without excess coadsorbed oxygen; figure detailing the primary identification of m/z 28 as neither ethane nor ethylene but CO; figure of yields corresponding to the selectivities in Figure 8; table detailing total coverage effects on reaction pathway; figure of detailed product appearance temperatures for high temperature reaction pathway; scheme for reaction mechanisms for minor products; and details for quantitative temperature-programmed reaction analysis including a table of correction factors, calculation of yield and selectivity, and fragmentation patterns for reactants and products. This material is available free of charge via the Internet at http://pubs.acs.org.

AUTHOR INFORMATION

Corresponding Author
*E-mail: rmadix@seas.harvard.edu.
Notes
The authors declare no competing financial interest.

ACKNOWLEDGMENTS

REFERENCES

(1) Gong, J.; Mullins, C. B. *Acc. Chem. Res.* **2009**, *42*, 1063−1073.

(2) Hashmi, A. S. K.; Hutchings, G. J. *Angew. Chem., Int. Ed.* **2006**, *45*, 7896−7936.

(3) Sinha, A. K.; Seelan, S.; Tsubota, S.; Haruta, M. *Top. Catal.* **2004**, *29*, 95−102.

(4) Huang, J.; Akita, T.; Faye, J.; Fujitani, T.; Takei, T.; Haruta, M. *Angew. Chem., Int. Ed.* **2009**, *48*, 7862−7866.

(5) Deng, X.; Friend, C. M. *J. Am. Chem. Soc.* **2005**, *127*, 17178−17179.

(6) Min, B. K.; Friend, C. M. *Chem. Rev.* **2007**, *107*, 2709−2724.

(7) Della Pina, C.; Falletta, E.; Rossi, M. *J. Catal.* **2008**, *260*, 384−386.

(8) Rodríguez-Reyes, J. C. F.; Friend, C. M.; Madix, R. J. *Surf. Sci.* **2012**, *606*, 1129−1134.

(9) Taarning, E.; Christensen, C. H. *Chim. Oggi* **2007**, *25*, 70−73.

(10) Christensen, C. H.; Jørgensen, B.; Rass-Hansen, J.; Egeblad, K.; Madsen, R.; Klitgaard, S. K.; Hansen, S. M.; Hansen, M. R.; Andersen, H. C.; Riisager, A. *Angew. Chem., Int. Ed.* **2006**, *45*, 4648−4651.

(11) Takei, T.; Iguchi, N.; Haruta, M. *Catal. Surv. Asia* **2011**, *15*, 80−88.

(12) Carrettin, S.; McMorn, P.; Johnston, P.; Griffin, K.; Kiely, C. J.; Attard, G. A.; Hutchings, G. J. *Top. Catal.* **2004**, *27*, 131−136.

(13) Prati, L.; Rossi, M. *J. Catal.* **1998**, *176*, 552−560.

(14) Bianchi, C.; Porta, F.; Prati, L.; Rossi, M. *Top. Catal.* **2000**, *13*, 231−236.

(15) Zhu, B.; Lazar, M.; Trewyn, B.; Angelici, R. *J. Catal.* **2008**, *260*, 1−6.

(16) Liu, P.; Li, C.; Hensen, E. J. M. *Chem. - Eur. J.* **2012**, *18*, 12122−12129.

(17) So, M. H.; Liu, Y.; Ho, C. M.; Che, C. M. *Chem. - Asian J.* **2009**, *4*, 1551−1561.

(18) Zhu, B.; Angelici, R. J. *Chem. Commun.* **2007**, *0*, 2157−2159.

(19) Nielsen, I. S.; Taarning, E.; Egeblad, K.; Madsen, R.; Christensen, C. H. *Catal. Lett.* **2007**, *116*, 35−40.

(20) Xu, B.; Liu, X.; Haubrich, J.; Madix, R. J.; Friend, C. M. *Angew. Chem., Int. Ed.* **2009**, *48*, 4206−4209.

(21) Wittstock, A.; Zielasek, V.; Biener, J.; Friend, C. M.; Bäumer, M. *Science* **2010**, *327*, 319−322.

(22) Liu, X.; Xu, B.; Haubrich, J.; Madix, R. J.; Friend, C. M. *J. Am. Chem. Soc.* **2009**, *131*, 5757−5759.

(23) Xu, B.; Haubrich, J.; Freyschlag, C. G.; Madix, R. J.; Friend, C. M. *Chem. Sci.* **2010**, *1*, 310−314.

(24) Xu, B.; Madix, R. J.; Friend, C. M. *J. Am. Chem. Soc.* **2010**, *132*, 16571−16580.

(25) Kosuda, K. M.; Wittstock, A.; Friend, C. M.; Bäumer, M. *Angew. Chem., Int. Ed.* **2012**, *51*, 1698−1701.

(26) Soulé, J.-F.; Miyamura, H.; Kobayashi, S. *J. Am. Chem. Soc.* **2011**, *133*, 18550−18553.

(27) Xu, B.; Zhou, L.; Madix, R. J.; Friend, C. M. *Angew. Chem., Int. Ed.* **2010**, *49*, 394−398.

(28) Siler, C. G. F.; Xu, B.; Madix, R. J.; Friend, C. M. *J. Am. Chem. Soc.* **2012**, *134*, 12604−12610.

(29) Klitgaard, S.; Egeblad, K.; Mentzel, U.; Popov, A.; Jensen, T.; Taarning, E.; Nielsen, I.; Christensen, C. *Green Chem.* **2008**, *10*, 419−423.

(30) Tanaka, S.; Minato, T.; Ito, E.; Hara, M.; Kim, Y.; Yamamoto, Y.; Asao, N. *Chem. - Eur. J.* **2013**, *19*, 11832−11836.

(31) Xu, B.; Madix, R. J.; Friend, C. M. *Chem. - Eur. J.* **2012**, *18*, 2313−2318.

(32) Xu, B.; Madix, R. J.; Friend, C. M. *Acc. Chem. Res.* **2014**, *47*, 761−772.

(33) Stowers, K. J.; Madix, R. J.; Friend, C. M. *J. Catal.* **2013**, *308*, 131−141.

(34) Xu, B.; Madix, R. J.; Friend, C. M. *J. Am. Chem. Soc.* **2011**, *133*, 20378−20383.

(35) Lukaski, A. C.; Barteau, M. A. *Catal. Lett.* **2009**, *128*, 9−17.

(36) Barteau, M.; Bowker, M.; Madix, R. *J. Catal.* **1981**, *67*, 118−128.

(37) Schubert, M. M.; Venugopal, A.; Kahlich, M. J.; Plzak, V.; Behm, R. J. *J. Catal.* **2004**, *222*, 32−40.

(38) Daté, M.; Okumura, M.; Tsubota, S.; Haruta, M. *Angew. Chem., Int. Ed.* **2004**, *43*, 2129−2132.

(39) Hao, Y.; Mihaylov, M.; Ivanova, E.; Hadjiivanov, K.; Knözinger, H.; Gates, B. C. *J. Catal.* **2009**, *261*, 137−149.

(40) Outka, D. A.; Madix, R. J. *Surf. Sci.* **1987**, *179*, 361−376.

(41) Outka, D.; Madix, R. *J. Am. Chem. Soc.* **1987**, *109*, 1708−1714.

(42) Gong, J.; Mullins, C. B. *J. Am. Chem. Soc.* **2008**, *130*, 16458−16459.

(43) Xu, B.; Haubrich, J.; Baker, T. A.; Kaxiras, E.; Friend, C. M. *J. Phys. Chem. C* **2011**, *115*, 3703−3708.

(44) Cremer, T.; Siler, C.; Rodriguez-Reyes, J. C.; Friend, C. M.; Madix, R. J. *J. Phys. Chem. Lett.* **2014**, *5*, 1126−1130.

(45) Ying, D.; Madix, R. J. *J. Catal.* **1980**, *61*, 48−56.

(46) Ying, D.; Madix, R. J. *J. Catal.* **1979**, *60*, 441−451.

(47) Yata, M.; Madix, R. J. *Surf. Sci.* **1995**, *328*, 171−180.

(48) Forbes, J. G.; Gellman, A. J. *J. Am. Chem. Soc.* **1993**, *115*, 6277−6283.

(49) Bent, B. E.; Nuzzo, R. G.; Dubois, L. H. *J. Am. Chem. Soc.* **1989**, *111*, 1634−1644.

(50) Quiller, R. G.; Baker, T. A.; Deng, X.; Colling, M. E.; Min, B. K.; Friend, C. M. *J. Chem. Phys.* **2008**, *129*, 064702.

(51) Xu, B.; Madix, R. J.; Friend, C. M. *Phys. Chem. Chem. Phys.* **2013**, *15*, 3179−3185.

(52) Paul, A. M.; Bent, B. E. *J. Catal.* **1994**, *147*, 264−271.

(53) Sault, A.; Madix, R. *Surf. Sci.* **1986**, *172*, 598−614.

(54) Brainard, R. L.; Madix, R. J. *J. Am. Chem. Soc.* **1989**, *111*, 3826−3835.

(55) Brainard, R. L.; Madix, R. J. *Surf. Sci.* **1989**, *214*, 396−406.

(56) Kretzschmar, I.; Levinson, J. A.; Friend, C. M. *J. Am. Chem. Soc.* **2000**, *122*, 12395−12396.

(57) Madix, R. J. *Surf. Sci.* **1994**, *299−300*, 785−797.